Journal of Molecular Catalysis B: Enzymatic 124 (2016) 77–82

Contents lists available at ScienceDirect

Journal of Molecular Catalysis B: Enzymatic

journal homepage: www.elsevier.com/locate/molcatb

One-pot enzymatic reaction sequence for the syntheses of D-glyceraldehyde 3-phosphate and L-glycerol 3-phosphate

Getachew S. Molla[a], Roland Wohlgemuth[b], Andreas Liese[a,*]

[a] Institute of Technical Biocatalysis, Hamburg University of Technology, Denickestr. 15, D-21073 Hamburg, Germany
[b] Sigma–Aldrich Chemie GmbH, Industriestr. 25, Buchs, CH-9470 Switzerland

ARTICLE INFO

Article history:
Received 24 July 2015
Received in revised form
18 November 2015
Accepted 4 December 2015
Available online 8 December 2015

Keywords:
Phosphorylated metabolite
One-pot reaction sequence
Reaction kinetics
Reactor simulation
Downstream processing

ABSTRACT

A one-pot enzymatic reaction sequence for the synthesis of optically pure D-glyceraldehyde 3-phosphate (D-GAP) and L-glycerol 3-phosphate (*sn*-G3P) was designed using fructose-bisphosphate aldolase from rabbit muscle (RAMA), *sn*-glycerol 3-phosphate dehydrogenase (*sn*-G3PDH) and formate dehydrogenase from *Candida boidinii* (FDH). The reaction sequence significantly improves the aldol cleavage of D-fructose 1,6-bisphosphate (D-F16BP) catalyzed by RAMA and yields 100% conversion of D-F16BP by overcoming thermodynamic limitation. The degradation kinetics of D-GAP under reaction conditions was investigated and a reaction kinetics model defining the entire cascade was developed. Validation of the model shows 98.5% correlation between experimental data and numerically simulated data matrices. The evaluation of different types of reactor was performed by combining the reaction kinetics model, mass balances and kinetics of the non-enzymatic degradation of D-GAP. Batch-wise operation in a stirred tank reactor (STR) is the most convenient procedure for the one-pot enzymatic syntheses of D-GAP and *sn*-G3P. The separation of the two products D-GAP and *sn*-G3P has been achieved using polyethylenimine (PEI)-cellulose TLC.

1. Introduction

In vitro synthesis of optically pure metabolites is of much interest in various applications such as enzyme substrates, biochemicals for biomedical research, drug discovery and the discovery of new metabolic pathways, standards for analytical technologies as well as pharmaceuticals and food additives. Phosphorylated metabolites have historically played a prominent role, are ubiquitous and are therefore highly required for various applications. In synthetic applications they are useful to design *in vitro* biocatalytic reaction sequences using various aldolases or transketolases that allow synthesizing novel products [1–12]. D-Glyceraldehyde 3-phosphate (D-GAP) and L-glycerol 3-phosphate (*sn*-G3P) are essential phosphorylated metabolites occurring in various metabolic pathways, *e.g.*, D-GAP is a central metabolite in glycolysis, thiamine biosynthesis [13], methylerythritol phosphate (MEP) pathway [14,15] and photosynthetis [16,17]. *sn*-G3P is a key building block of phospholipids in bacteria as well as eucarya and useful for an *in vitro* preparation of optically pure α-glycerophospholipids that can be tailored with a desired fatty acid chain length and acyl-number as well as position using *sn*-glycerol 3-phosphate *O*-acyltransferase [18–23]. The therapeutic effect of calcium glycerol phosphate has recently been reported for preserving and/or treating of intestinal integrity in ischemia [24,25].

Phosphorylation of glycerol by ATP catalyzed by glycerol kinase (E.C. 2.7.1.30) has been reported as a major enzymatic synthesis of *sn*-G3P [26,27]. As this reaction system requires stoichiometric amounts of the phosphoryl donor ATP, the scalability of this reaction system for large-scale synthesis is limited. The scalability of most reported ATP regeneration systems, which require more expensive co-substrates like phosphoenolpyruvate [1,26,28] and acetyl phosphate [1,27,29], is even more limited. Several multistep chemical synthetic routes have been reported for the preparation of D-GAP, *e.g.*, a 9 step sequence starting from a kilogram of D-mannitol to produce few grams of D-GAP using toxic reagents like $HgCl_2$ and HgO [30], a 10 step sequence starting from 2-*O*-benzyl-D-arabinose [31], oxidation of D-fructose 6-phosphate (D-F6P) by $Pb(OAc)_4$ [10,32], oxidative cleavage by H_5IO_6 of D-fructose 1,6-bisphosphate (D-F16BP) [33] or of D-F6P [28]. Lack of selectivity makes purification steps too laborious and drastically reduces product yields. The reported enzymatic synthesis of D-GAP applying aldolase to catalyze aldol cleavage of D-F16BP [34] has thermodynamics as main drawback, being in favor of reverse aldol condensation with an equilibrium constant of nearly 10^{-4} M [2,35]. To overcome this

* Corresponding author at: Institute of Technical Biocatalysis, Hamburg University of Technology (TUHH), Denickestr. 15, Hamburg D-21073, Germany. Fax: +49 40428 78 2127.
E-mail address: liese@tuhh.de (A. Liese).

http://dx.doi.org/10.1016/j.molcatb.2015.12.004
1381-1177/

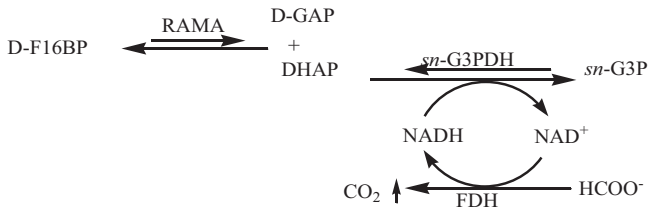

Fig. 1. A one-pot cascade enzymatic reaction sequence for the syntheses of D-GAP and *sn*-G3P; D-F16BP: D-fructose 1,6-bisphosphate, D-GAP: D-glyceraldehyde 3-phosphate, DHAP: dihydroxyacetone phosphate, RAMA: rabbit muscle aldolase, *sn*-G3P: *sn*-glycerol 3-phosphate, *sn*-G3PDH: *sn*-glycerol 3-phosphate dehydrogenase and FDH: formate dehydrogenase.

Table 1
Activity and stability of RAMA, *sn*-G3PDH and FDH as a function of pH: 0.5 mM D-F16BP, 0.5 mM NADH, 0.18 U/ml RAMA and 6.4 U/ml *sn*-G3PDH (for the activity assay of RAMA); 0.5 mM DHAP, 0.5 mM NADH and 0.8 U/ml *sn*-G3PDH (for the activity assay of *sn*-G3PDH) and 50 mM NaHCOO, 0.5 mM NAD^+ and 6.5 U/ml FDH (for the activity assay of FDH) in 50 mM TEA buffer at 25 °C. Incubation conditions: RAMA (50 mM TEA buffer, 25 °C and 400 rpm); *sn*-G3PDH (50 mM TEA buffer, 25 °C and 400 rpm) and FDH (50 mM TEA buffer, 25 °C and 400 rpm).

Enzyme	Maximum activity	Loss of activity	Higher stability
RAMA	At pH 6	11% at pH 7 and 35% at pH 8	At pH [7,8]
sn-G3PDH	At pH 8	88% at pH 6 and 45% at pH 7	At pH [6–9]
FDH	At pH [7–9]	0% at pH 8	At pH [6–8]

limitation by shifting the reaction equilibrium, the reaction was carried out in the presence of hydrazine yielding D-GAP hydrazone as final product instead of the desired D-GAP [34].

In consequence three main objectives of this work were defined, starting with the design of a one-pot enzymatic reaction sequence for the syntheses of D-GAP and *sn*-G3P without protection and deprotection steps. The second objective was a comprehensive reaction engineering characterization like activity, stability and selectivity of all enzymes involved, stability of cofactors and products, reaction kinetics model development and simulation of different reactor types. To develop a downstream processing (DSP) method was the third objective. In the synthesis of D-GAP, fructose-bisphosphate aldolase from rabbit muscle (RAMA) (E.C. 4.1.2.13) catalyzed aldol cleavage of D-F16BP to D-GAP and dihydroxyacetone phosphate (DHAP) was used. *In situ* reduction of the co-product DHAP to *sn*-G3P catalyzed by *sn*-glycerol 3-phosphate dehydrogenase from rabbit muscle (*sn*-G3PDH) (E.C. 1.1.99.5) was added as consecutive reaction step in order to shift the reaction equilibrium and synthesize the second target product (*sn*-G3P). Moreover, since the second reaction step requires the expensive cofactor NADH, it was coupled with formate dehydrogenase from *Candida boidinii* (FDH) (E.C. 1.2.1.2) catalyzing the *in situ* regeneration of NADH. The entire reaction sequence is shown in Fig. 1.

2. Results and discussion

2.1. Reaction system optimization

The capability of the one-pot reaction sequence (shown in Fig. 1) to shift the reaction equilibrium of RAMA catalyzed aldol cleavage of D-F16BP was examined by performing reactions using excess amount of NADH without coupling the cofactor regeneration system. Results showed a significant improvement with reactions yielding 100% conversions of D-F16BP. The selection of optimum reaction conditions like pH is essential for developing an enzymatic process and a reaction kinetics model. Activities, stabilities and selectivities of all three enzymes involved, stabilities of both the reduced and oxidized nucleotide cofactor as well as stability of D-GAP as a function of pH were investigated. Table 1 shows activity

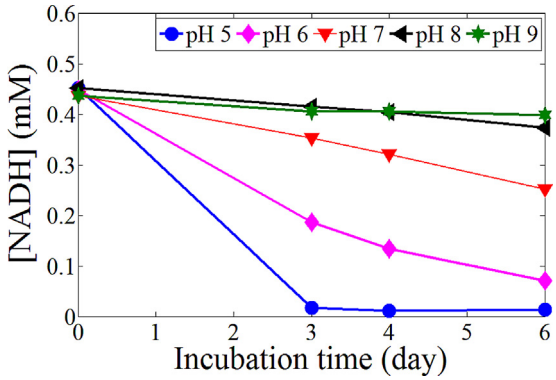

Fig. 2. Stability of NADH incubated in 50 mM TEA at 25 °C at different pH levels.

and stability data of all the three enzymes involved in the reaction sequence as a function of pH; moreover, detailed enzymes activity and stability data are shown in the supplementary document. Considering that enzymes show maximum activity at different pH, the activity loss of one enzyme at a pH where another enzyme shows maximum activity and the different enzyme stabilities with respect to pH, pH 8 appears to represent an optimum value.

As shown in Fig. 2 and it has also been known that the reduced form of the nucleotide cofactor (NADH) is unstable at acidic pH, while it is stable at alkaline pH [36]. The oxidized form of the nucleotide cofactor (NAD^+) is on the other hand unstable at alkaline pH, while it is stable at acidic pH [36]. The decrease of pH accelerates NADH depletion, whereas the increase of pH accelerates NAD^+ depletion. According to results of stability measurements for NADH as well as for NAD^+ [36], as function of pH, pH 8 appears to be optimum for the stability of NADH and NAD^+.

The stabilities of triosephosphate metabolites such as DHAP and D-GAP at neutral and alkaline pH conditions depend very much on the molecular structure, *e.g.*, whether the glyceraldehyde is phosphorylated in the 2- or 3-position, and the medium composition [1,28]. A decomposition mechanism of eliminating the phosphate group via an enediolate phosphate intermediate has been proposed [37,38]. D-GAP is stable at pH of 4 or below while the enzymes involved are not active and NADH shows a very low stability at this pH region; therefore, the degradation kinetics of D-GAP at pH 8 is a critical parameter for process optimization of the one-pot enzymatic reaction sequence. The degradation rate of D-GAP in 50 mM TEA buffer at pH 8 and 25 °C can be defined by first order kinetics with a rate constant of $2.3 \times 10^{-5}\ s^{-1}$ and a corresponding half-life time of 8.35 h. The degradation of D-GAP was investigated in different buffer media because catalysis of the phosphate elimination reaction by a tertiary amine buffer and a rate increase with increasing buffer concentration was described [37]. Our experiments show the rates of D-GAP degradation in non-buffered aqueous medium, 100 mM TEA, 50 mM TEA and 100 mM potassium phosphate buffer (PPB) media to be similar, while D-GAP stability is increased in 100 mM Tris–HCl buffer. Fig. 3 shows the degradation of D-GAP incubated in different buffer media at pH 8. The stabilization of D-GAP by Tris–HCl buffer may be due to interactions of D-GAP with the Tris–HCl buffer [39]. Tris–HCl buffer is however not applicable as it also affects the activity of *sn*-G3PDH due to interactions with DHAP and additionally the use of inorganic phosphate buffer interferes in product purification. Furthermore, the selectivity of *sn*-G3PDH toward D-GAP and DHAP due to their structural similarity as well as the NADH oxidase activity of all the three enzymes active in the reaction sequence were examined. Results demonstrate 100% *sn*-G3PDH selectivity toward to DHAP and no depletion of NADH in the presence of all the three enzymes without D-F16BP addition.

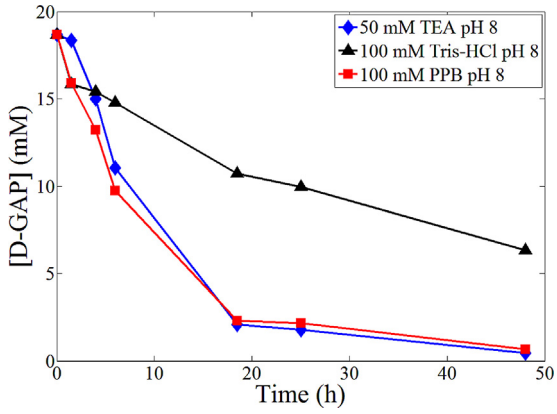

Fig. 3. Degradation of 20 mM D-glyceraldehyde 3-phosphate incubated in 50 mM TEA buffer pH 8, 100 mM Tris–HCl buffer pH 8 or alternatively 100 mM potassium phosphate buffer (PPB) pH 8 at 25 °C.

Table 2
The influence of co-substances present in the reaction mixture on the activity of rabbit muscle aldolase (RAMA), *sn*-glycerol 3-phosphate dehydrogenase (*sn*-G3PDH) and formate dehydrogenase (FDH) involved in the reaction sequence.

Co-substance	RAMA	*sn*-G3PDH	FDH
D-F16BP	Native	×	×
D-GAP	Native	√	×
sn-G3P	×	Native	×
NaHCOO	×	√	Native

√Indicates the co-substance suppresses the enzyme activity; ×indicates the co-substance does not influence the enzyme activity.

2.2. Reaction kinetics model development

The investigation of biocatalytic reaction kinetics is essential for identifying relevant kinetic parameters and to understand the reaction mechanism. An appropriate reaction kinetics model is a major tool and criterion to choose a specific reactor type and to optimize the process [40–42]. Since the reaction sequence contains, in addition to the native substrate and product of each of the enzymes, several compounds, their influence on each of the enzyme activities was investigated. These activity data can be included in the overall reaction kinetics model and are useful for selecting the concentration of each enzyme. Table 2 shows the influence on the activity of enzymes involved. The dependence of the enzyme activities on the concentrations of their native substrates and products has been analyzed as well and taken into account in the development of kinetic models.

The cascade reaction consists of three enzymes arranged in two reversible consecutive reactions and the last one coupled with the third irreversible cofactor regeneration. For the development of the overall reaction kinetics model, this simplifies the entire reaction sequence to a single substrate irreversible enzymatic reaction. The kinetic behavior of each enzyme with respect to their native substrate and product must be known in order to choose the appropriate enzyme and substrate concentrations as well as the enzyme ratios. We therefore identified and determined the relevant kinetic parameters for all the three enzymes. The kinetic constants were determined by rearranging the non-linear rate responses of the enzymes as a function of concentrations into a linear form using double reciprocal (Lineweaver–Burk) and its secondary plot methods. Table 3 shows the kinetic properties and values of the kinetic constants for RAMA, FDH and *sn*-G3PDH with respect to their native substrates and products.

The mathematical models shown in Eqs. (1) and (2) were developed for FDH and RAMA kinetics, respectively. The effect of DHAP was not considered in the rate equation for the RAMA-catalyzed

Table 3
Kinetic properties and the values of kinetic constants for rabbit muscle aldolase (RAMA), formate dehydrogenase (FDH) and *sn*-glycerol 3-phosphate dehydrogenase (*sn*-G3PDH).

Kinetics parameters	RAMA	FDH	*sn*-G3PDH
$K_{m,D\text{-}F16BP}$ (mM)	0.0065 ± 0.002		
$K_{ic,D\text{-}GAP}$ (mM)	0.11		
$K_{iu,D\text{-}GAP}$ (mM)	0.40		
v_{max} (U/mg)	6.80 ± 0.2		
$K_{m,HCOO^-}$ (mM)		6.08 ± 2.2	
K_{m,NAD^+} (mM)		0.02 ± 0.001	
$K_{ic,NADH}$ (mM)		0.04 ± 0.01	
v_{max} (U/mg)		0.55 ± 0.005	
$K_{m,DHAP}$ (mM)	0.049 [43]		0.28
$K_{m,NADH}$ (mM)			0.0081 [44]
v_{max} (U/mg)			123

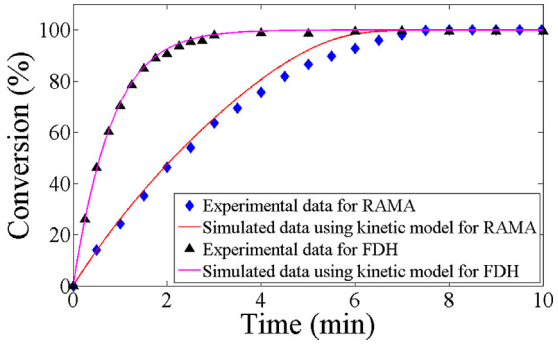

Fig. 4. Graphical fitness of experimental data and numerically simulated data using the kinetics models for batch reactions of RAMA catalyzed aldol cleavage of D-F16BP and FDH catalyzed reduction of NAD^+: 0.1 mM D-F16BP, 0.5 mM NADH, 0.0046 mg/ml RAMA, 0.044 mg/ml *sn*-G3PDH in 50 mM TEA pH 8 and 25 °C for RAMA catalyzed aldol cleavage of D-F16BP and 0.0125 mM NAD^+, 500 mM NaHCOO, 0.075 mg/ml FDH in 50 mM TEA pH 8 and 25 °C for FDH catalyzed reduction of NAD^+.

aldol cleavage of D-F16BP, as it is reduced *in-situ* to *sn*-G3P. RAMA is non-competitively inhibited by D-GAP. The smaller competitive inhibition constant ($K_{ic,D\text{-}GAP}$) compared to the un-competitive inhibition constant ($K_{iu,D\text{-}GAP}$) suggests that D-F16BP and D-GAP impede each other in forming a complex with the active site of RAMA. The kinetic models were validated by simulating the time course of several batch conversions at different starting substrate and enzyme concentrations using Matlab®. Evaluations of the experimental data and the numerically simulated data matrices show for the models of FDH and RAMA a 98.8% and 98.5% 2-D correlation, respectively. Graphical correlations between experimental and numerically simulated conversions versus reaction time for both models are shown in Fig. 4.

$$v_1 = v_{max} \times \frac{[NAD^+]}{K_{m,NAD^+} \times \left(1 + [NADH]/K_{ic,NADH}\right) + [NAD^+]} \times \frac{[HCOO^-]}{K_{m,HCOO^-} + [HCOO^-]} \quad (1)$$

The overall model for the reaction kinetics can be developed by fixing one of the reaction steps as rate limiting. The rate limiting step can be adjusted by knowing the kinetics behavior of each of the enzymes and choosing an appropriate enzyme ratio. In our case the RAMA-catalyzed aldol cleavage of D-F16BP was set to be the rate limiting step for the purpose of simplification and to avoid the accumulation of D-GAP in the reaction solution. It is thus essential to maintain the *sn*-G3PDH-catalyzed reduction of DHAP at a higher rate than the RAMA-catalyzed aldol cleavage of D-F16BP in order to suppress the reverse aldol condensation reaction and to pre-

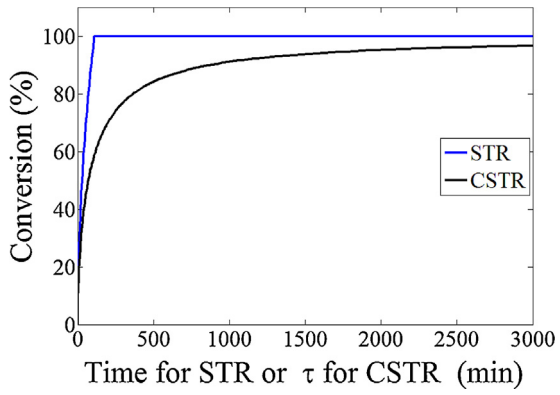

Fig. 5. Comparison of stirred tank reactor (STR) and continuously operated stirred reactor (CSTR) based on conversion as a function of reaction time for STR or residence time for CSTR for the syntheses of D-GAP and *sn*-G3P: 5 mM D-F16BP, 0.5 mM NADH, 50 mM NaHCOO, 0.15 mg/ml RAMA, 1.43 mg/ml *sn*-G3PDH, 3.7 mg/ml FDH in 50 mM TEA buffer pH 8 and 25 °C.

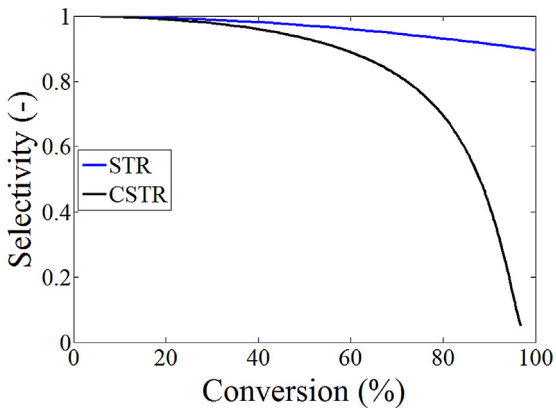

Fig. 6. Comparison of stirred tank reactor (STR) and continuously operated stirred reactor (CSTR) based on selectivity as a function conversion for the syntheses of D-GAP and *sn*-G3P: 5 mM D-F16BP, 0.5 mM NADH, 50 mM NaHCOO, 0.15 mg/ml RAMA, 1.43 mg/ml *sn*-G3PDH, 3.7 mg/ml FDH in 50 mM TEA buffer pH 8 and 25 °C.

vent the effect of DHAP on the activity of RAMA. Additionally, the FDH-catalyzed NADH regeneration must be adjusted to a higher rate than the *sn*-G3PDH-catalyzed reduction of DHAP so that *sn*-G3PDH activity is not affected by NADH shortage. Therefore, the overall reaction kinetics is simplified to a *uni-uni* irreversible enzymatic reaction and can be defined using the reaction kinetics model developed for RAMA shown in the following Eq. (2).

$$v_2 = v_{\max} \times \frac{[\mathrm{D-F16BP}]}{K_{m,\mathrm{D-F16BP}} \times \left(1 + [\mathrm{D-GAP}]/K_{\mathrm{ic,D-GAP}}\right) + [\mathrm{D-F16BP}] \times \left(1 + [\mathrm{D-GAP}]/K_{\mathrm{iu,D-GAP}}\right)} \quad (2)$$

2.3. Selection of an appropriate reactor type and separation method development

The performance of different reactor modes of operation was evaluated by combining the developed reaction kinetics model, mass balances of reactors and kinetics of the non-enzymatic decomposition of D-GAP. The performance of the reactors was evaluated using the parameters such as conversion, selectivity, space-time yield (STY) and specific productivity. Eqs. (3) and (4) show differential equations for the simulation of D-F16BP and D-GAP concentrations for batch-wise mode of operation in a stirred tank reactor (STR), respectively. Eqs. (5) and (6) show steady state differential equations for the simulation of D-F16BP and D-GAP concentrations for a continuous mode of operation in a continuously operated stirred tank reactor (CSTR), respectively. [D − F16BP]o and [D − F16BP] represent influx and efflux concentrations in CSTR, respectively. [D − GAP]o and [D − GAP] represent influx into the CSTR, which is negligible, and efflux, respectively. As can be seen, Eqs. (4) and (6) include the kinetics of D-GAP decay at the reaction conditions assuming the unit of reaction time and residence time in hour.

$$\frac{\partial[\mathrm{D-F16BP}]}{\partial t} = [\mathrm{RAMA}](-v_2) \quad (3)$$

$$\frac{\partial[\mathrm{D-GAP}]}{\partial t} = [\mathrm{RAMA}](v_2) \times e^{-0.083t} \quad (4)$$

$$\frac{\partial[\mathrm{D-F16BP}]}{\partial t} = \frac{([\mathrm{D-F16BP}]\mathrm{o} - [\mathrm{D-F16BP}])}{\tau} - [\mathrm{RAMA}]\,v_2 \quad (5)$$

$$\frac{\partial[\mathrm{D-GAP}]}{\partial t} = \left(\frac{([\mathrm{D-GAP}]\mathrm{o} - [\mathrm{D-GAP}])}{\tau} + [\mathrm{RAMA}]\,v_2\right) \times e^{-0.083\tau} \quad (6)$$

Fig. 5 shows a comparison of the batch-wise operation in a stirred tank reactor (STR) and the continuous operation in a continuously operated stirred tank reactor (CSTR) based on conversion. Conversion is defined as the number of D-F16BP molecules converted per starting D-F16BP molecules. As can be seen in Fig. 5 higher conversion in a short time can be achieved via STR, *e.g.*, in order to achieve a comparable conversion of 95% in the same reaction time for STR and residence time for CSTR, the CSTR requires a 20-fold higher amount of enzyme than the STR.

Fig. 6 shows that the STR shows a better selectivity performance than the CSTR. Selectivity is defined as the number of D-GAP molecules synthesized per number of D-F16BP molecules converted. For the synthesis of D-GAP, selectivity is a useful parameter due to the exponential decay of D-GAP with time at pH 8. The selectivity performance of the reactors was evaluated as a function of conversion using the same amount of enzymes.

Inhibition of RAMA by D-GAP leads in the case of the CSTR to a low steady-state reaction rate. Using conditions given in Figs. 5 and 6 at the same conversion of 95% STR offers STY of 10.56 $gL^{-1}\,day^{-1}$ while the STY of CSTR drops to 0.08 $gL^{-1}\,day^{-1}$ due to their selectivity difference. Therefore, the most convenient reactor type for the one-pot cascade enzymatic syntheses of D-GAP and *sn*-G3P is the STR, due to the gradual increase of product with reaction time. The separation of D-GAP and *sn*-G3P was achieved by using TLC containing the strong basic anion exchanger polyethylenimine (PEI)-cellulose and by considering D-GAP stability in the optimization of developing solvent and pH. A solution of 1 M KCl dissolved in 100 mM HCl pH 2 was selected for high separation ability and stability of D-GAP. An excellent separation of D-GAP (R_f of 0.2) and *sn*-G3P (R_f of 0.9) has been achieved. Up-scaling the TLC separation methodology to preparative column chromatography scale is however hindered by a current commercial none availability of the polyethylenimine (PEI)-cellulose material. Preparation of polyethylenimine (PEI)-cellulose material is therefore in the interest of our research in order to scale-up the designed reaction sequence to preparative scale.

3. Conclusions

A one-pot enzymatic reaction sequence has been designed for preparing D-GAP and *sn*-G3P. The reaction sequence shows a sig-

nificant improvement of the RAMA-catalyzed aldol cleavage of D-F16BP yielding 100% conversion of D-F16BP. Detailed characterizations of the enzymatic reaction sequence were performed. The degradation rates of D-GAP in 50 mM TEA buffer at pH 8 and 25 °C was measured. First order kinetic rate constant of 2.3×10^{-5} s^{-1} and half-life of 8.35 h have been determined. D-GAP has been found to show higher stability in Tris–HCl buffer.

Each of the three enzymes involved in the reaction sequence was investigated regarding kinetic behavior in order to choose the appropriate enzyme and substrate concentrations and enzyme ratios. RAMA is non-competitively inhibited by D-GAP and the competitive and un-competitive inhibition constants suggest that D-F16BP and D-GAP impede each other for complexation with the active site of RAMA. The reaction kinetics models were validated by simulating the time course of several batch reactions. The performance of different reactor modes of operation for the enzymatic reaction sequence was evaluated by combining the developed reaction kinetics model, mass balances of reactors and kinetics of the non-enzymatic decomposition of D-GAP. Batch-wise operation in a STR is the most convenient process for the one-pot enzymatic syntheses of D-GAP and *sn*-G3P. Alternative to STR, continuous operation using packed bed reactor (PBR) can be applied due to the gradual increase of the inhibitory product across the length of the reactor. However, in this study, homogenous soluble enzymes were used and a strategy to use three immobilized enzymes often shows low efficiency due to mass transport limitations. The separation of D-GAP and *sn*-G3P has been achieved using polyethylenimine (PEI)-cellulose TLC. Preparation of polyethylenimine (PEI)-cellulose material is in the interest of our research in order to scale-up the TLC separation methodology to preparative column chromatography scale.

4. Experimental

4.1. Materials

Ammonium molybdate, anthranilic acid, ascorbic acid, D-fructose 1,6-bisphosphate (D-F16BP) D-glyceraldehyde 3-phosphate, *sn*-glycerol 3-phosphate bis(cyclohexylammonium) salt, reduced form of β-nicotinamide adenine dinucleotide disodium salt, oxidized form of β-nicotinamide adenine dinucleotide disodium salt, sodium formate, fructose-bisphosphate aldolase from rabbit muscle (RAMA), *sn*-glycerol 3-phosphate dehydrogenase (*sn*-G3PDH) from rabbit muscle, formate dehydrogenase from *C. boidinii* (FDH), were purchased from Sigma–Aldrich GmbH (Buchs, Switzerland). Nitric acid (65%), potassium chloride, hydrochloric acid, potassium dihydrogen phosphate, methanol and triethanolamine were purchased from Carl Roth GmbH (Karlsruhe, Germany). All chemicals and solvents were used without further purification. Polyethylenimine (PEI) cellulose strong basic anion exchange TLC plate was purchased from Merck KGaA (Darmstadt, Germany).

4.2. Analytics

All activity measurements were carried out using an UVIKON spectrophotometer by measuring changes in NADH concentration at 340 nm. The concentrations of D-GAP was analyzed by HPLC (Agilent 1100, Hewlett Packard) on a Eurokat-H column (300 mm × 8 mm, Knauer) with 5 mM H_2SO_4 as eluent at a flow rate of 0.5 ml/min and 75 °C, using a refractive index detector at 35 °C. Typical retention time for D-GAP is 9.8 ± 0.2 min.

4.3. Methods

A solution containing 0.5 mM D-F16BP and 0.5 mM NADH was prepared in 50 mM TEA buffer for the activity assays of RAMA as a function of pH. The reactions were started by the addition of required amount of *sn*-G3PDH followed by 0.004 mg/ml of RAMA so that RAMA catalyzed aldol cleavage of D-F16BP is rate limiting. A substrate solution of 0.5 mM DHAP and 0.5 mM NADH was prepared in 50 mM TEA buffer and used to assay the activity of *sn*-G3PDH as a function of pH. All reactions were started by the addition of 0.8 U/ml of *sn*-G3PDH. For the activity assay of FDH as a function of pH, a substrate solution of 50 mM NaHCOO and 0.5 mM NAD^+ was prepared in 50 mM TEA buffer and all reactions were started by the addition of 0.075 mg/ml of FDH. The long term operational stabilities of RAMA, *sn*-G3PDH and FDH were examined by incubating the enzymes in 50 mM TEA buffer at different pH from 5 to 9 and 25 °C. The remaining activities were routinely analyzed with the assays described above for the activity measurements as a function of pH. The stability of D-GAP was examined by incubating 20 mM of D-GAP prepared in non-buffered medium, 100 mM TEA, 50 mM TEA, 100 mM Tris–HCl and 100 mM PPB buffer pH 8 at 25 °C. The degradation of D-GAP was analyzed via HPLC.

The capability of the reaction sequence to shift the equilibrium was demonstrated by performing a batch reaction using a substrate solution of 0.25 mM D-F16BP and 0.5 mM NADH prepared in 50 mM TEA buffer pH 8. The reaction was started by the addition of 0.044 mg/ml of *sn*-G3PDH and 0046 mg/ml of RAMA with respective order. Two batch reactions using 0.25 mM and 0.5 mM D-GAP, both containing 0.5 mM NADH, for checking the selectivity of *sn*-G3PDH toward D-GAP and *sn*-G3P were carried out in 50 mM TEA pH 8 and 25 °C. Activity measurements as function of co-substance concentrations were carried out in 50 mM TEA pH 8 and 25 °C. Linear representations of Michaelis–Menten enzyme kinetics equation were applied in order to determine the values of kinetics parameters. Separation of D-GAP and *sn*-G3P by using polyethylenimine (PEI)-cellulose strong basic anion exchange TLC plate was performed using 1 M KCl dissolved in 100 mM HCl pH 2 as a developing solvent. A staining solution containing 0.01 g/ml of ammonium molybdate, 0.01 g/ml of ascorbic acid and 0.01 g/ml of anthranilic acid was prepared in 65% nitric acid:methanol (1:9, V/V) using a method as described elsewhere [45].

Acknowledgment

We would like to thank the German Federal Ministry of Education and Research (BMBF) for financing the project P28 under the cluster of Biocatalysis2021.

Appendix A. Supplementary data

Supplementary data associated with this article can be found, in the online version, at http://dx.doi.org/10.1016/j.molcatb.2015.12.004.

References

[1] C.H. Wong, G.M. Whitesides, J. Org. Chem. 48 (1983) 3199–3205.
[2] M.D. Bednarski, E.S. Simon, N. Bischofberger, W.D. Fessner, M.J. Kim, W. Lees, T. Saito, H. Waldmann, G.M. Whitesides, J. Am. Chem. Soc. 111 (1989) 627–635.
[3] W.-D. Fessner, G. Sinerius, Angew. Chem. Int. Ed. Engl. 33 (1994) 209–212.
[4] I. Sánchez-Moreno, V. Hélaine, N. Poupard, F. Charmantray, B. Légeret, L. Hecquet, E. García-Junceda, R. Wohlgemuth, C. Guérard-Hélaine, M. Lemaire, Adv. Synth. Catal. 354 (2012) 1725–1730.
[5] R. Schoevaart, F. van Rantwijk, R.A. Sheldon, J. Org. Chem. 65 (2000) 6940–6943.
[6] R. Wohlgemuth, Biocatal. Biotransform. 26 (2008) 42–48.
[7] R. Wohlgemuth, ChemInform 41 (2010) 23–29.
[8] O.M. Rosen, P. Hoffee, B.L. Horecker, J. Biol. Chem. 240 (1965) 1517–1524.
[9] E. Racker, J. Biol. Chem. 196 (1952) 347–365.
[10] H. Li, J. Tian, H. Wang, S.-Q. Yang, W.-Y. Gao, HCA 93 (2010) 1745–1750.
[11] Z. Li, L. Cai, M. Wei, P.G. Wang, Carbohydr. Res. 357 (2012) 143–146.
[12] P. Knochel, G.A. Molander, Comprehensive Organic Synthesis, Elsevier Science, 2014.

[13] C.T. Jurgenson, T.P. Begley, S.E. Ealick, Annu. Rev. Biochem. 78 (2009) 569–603.
[14] M. Rohmer, Pure Appl. Chem. 79 (2007) 739–751.
[15] L. Zhao, W.-C. Chang, Y. Xiao, H.-W. Liu, P. Liu, Annu. Rev. Biochem. 82 (2013) 497–530.
[16] L. Dijkhuizen, W. Harder, Antonie Van Leeuwenhoek 50 (1984) 473–487.
[17] T. Hasunuma, K. Harada, S.-I. Miyazawa, A. Kondo, E. Fukusaki, C. Miyake, J. Exp. Bot. 61 (2010) 1041–1051.
[18] H.J. Fallon, R.G. Lamb, J. Lipid Res. 9 (1968) 652–660.
[19] E.E. Hill, D.R. Husbands, E.M. Lands William, J. Biol. Chem. 243 (1968) 4440–4451.
[20] E. Mårtensson, J. Kanfer, J. Biol. Chem. 243 (1968) 497–501.
[21] H.M. Abou-Issa, W.W. Cleland, Biochim. Biophys. Acta Lipids Lipid Metab. 176 (1969) 692–698.
[22] R.G. Lamb, H.J. Fallon, J. Biol. Chem. 245 (1970) 3075–3083.
[23] T.K. Ray, J.E. Cronan, R.D. Mavis, P.R. Vagelos, J. Biol. Chem. 245 (1970) 6442–6448.
[24] P. Datta, M.T. Weis, World J. Gastroenterol. 21 (2015) 9055–9066.
[25] A.E. Kligerman, M.T. Weis, Methods and compositions of treating and preventing intestinal injury and diseases related to tight junction dysfunction, Google Patents, WO2014130678 A2, 2014.
[26] D.C. Crans, G.M. Whitesides, J. Am. Chem. Soc. 107 (1985) 7019–7027.
[27] V.M. Rios-Mercadillo, G.M. Whitesides, J. Am. Chem. Soc. 101 (1979) 5828–5829.
[28] D. Gauss, B. Schoenenberger, R. Wohlgemuth, Carbohydr. Res. 389 (2014) 18–24.
[29] G.M. Whitesides, M. Siegel, P. Garrett, J. Org. Chem. 40 (1975) 2516–2519.
[30] C.E. Ballou, O.L. Fischer Hermann, J. Am. Chem. Soc. 77 (1955) 3329–3331.
[31] Gary R. Gray, Robert Barker, Carbohydr. Res. 20 (1971) 31–37.
[32] A.S. Serianni, J. Pierce, R. Barker, Biochemistry 18 (1979) 1192–1199.
[33] A. Szewczuk, E. Wolny, M. Wolny, T. Baranowski, Acta Biochim. Pol. 8 (1961) 201–207.
[34] Leo M. Hall, Biochem. Biophys. Res. Commun. 3 (1960) 239–243.
[35] A. Flamholz, E. Noor, A. Bar-Even, R. Milo, Nucleic Acids Res. 40 (2012) D770–D775.
[36] O.H. Lowry, J.V. Passonneau, M.K. Rock, J. Biol. Chem. 236 (1961) 2756–2759.
[37] J.P. Richard, Biochem. Soc. Trans. 21 (1993) 549–553.
[38] S.A. Phillips, P.J. Thornalley, Eur. J. Biochem. 212 (1993) 101–105.
[39] W.A. Bubb, H.A. Berthon, P.W. Kuchel, Bioorg. Chem. 23 (1995) 119–130.
[40] M. Biselli, U. Kragl, C. Wandrey, Enzyme Catalysis in Organic Synthesis, in: K. Drauz, H. Waldmann (Eds.), Wiley-VCH Verlag GmbH, Weinheim, Germany, 2002, pp. 185–257.
[41] J. Brass, F. Hoeks, M. Rohner, J. Biotechnol. 59 (1997) 63–72.
[42] D. Vasic-Racki, J. Bongs, U. Schörken, G.A. Sprenger, A. Liese, Bioprocess Biosyst. Eng. 25 (2003) 285–290.
[43] M. Callens, D.A. Kuntz, F.R. Opperdoes, Mol. Biochem. Parasitol. 47 (1991) 1–9.
[44] P. Bentley, F.M. Dickinson, I.G. Jones, Biochem. J. 135 (1973) 853–859.
[45] B.R. Bochner, D.M. Maron, B.N. Ames, Anal. Biochem. 117 (1981) 81–83.